

ORIGINAL ARTICLE

Aloe emodin exerts potent anticancer effects in MIA PaCa-2 and PANC-1 human pancreatic adenocarcinoma cell lines through activation of both apoptotic and autophagic pathways, sub-G1 cell cycle arrest and disruption of mitochondrial membrane potential ($\Delta\Psi_m$)

Yiqun Du^{1,2}, Jian Zhang^{1,2}, Zhonghua Tao^{1,2}, Chenchen Wang^{1,2}, Shiyan Yan³, Xiaowei Zhang^{1,2}, Mingzhu Huang^{1,2}

¹Department of Medical Oncology, Fudan University Shanghai Cancer Center, Shanghai 200032, China; ²Department of Oncology, Shanghai Medical College, Fudan University, Shanghai 200032, China; ³Department of Gastroenterology, Xinhua Hospital, Shanghai Jiaotong University, School of Medicine, Shanghai 200092, China.

Summary

Purpose: To study the anticancer effects of aloe emodin against the MIA PaCa-2 and PANC-1 human pancreatic adenocarcinoma cancer cell lines by evaluating its effect on autophagic cell death, mitochondrial membrane potential ($\Delta\Psi_m$) loss and cell cycle arrest.

Methods: The MTT assay was employed to examine the anti-proliferative effect of aloe emodin on these cells, and inverted phase contrast and fluorescence microscopes were used to evaluate apoptotic induction. Flow cytometry was performed to examine the effects of aloe emodin on $\Delta\Psi_m$ and cell cycle phase distribution.

Results: The findings indicated that aloe emodin induced dose-dependent cytotoxicity in both pancreatic carcinoma cells with MIA PaCa-2 cells being more susceptible than PANC-1, along with inhibiting cancer cell colony formation. Aloe emodin-treated cells exhibited cell shrinkage along with distortion of the normal cell morphology. In addition, these cells showed chromatin condensation, membrane blebbing and predominantly emitted red fluorescence, which signi-

fied apoptosis. Following treatment with aloe emodin (10, 40 and 80 μ M) the early apoptotic cell percentage increased to 17.5, 39.6 and 58.8%, respectively, while late apoptotic cells percentage increased to 22.3, 27.6 and 37.2% respectively. There was also a marked increase in the loss of $\Delta\Psi_m$ in the aloe emodin-treated cells, as well as dose-dependent sub-G₁ cell cycle arrest. Furthermore, aloe emodin treatment led to a substantial enhancement of the conversion of light chain 3 (LC3)-I to LC3-II and this increase was shown to follow aloe emodin dose-dependent pattern, thus indicating that aloe emodin may induce autophagy in addition to apoptosis.

Conclusion: To sum up, aloe emodin inhibits cancer cell growth in human pancreatic carcinoma cells and it was shown that these anticancer effects are mediated via both apoptotic and autophagic pathways, cell cycle arrest and loss of mitochondrial membrane potential.

Key words: aloe emodin, autophagy, cell cycle arrest, flow cytometry, pancreatic cancer

Introduction

Pancreatic cancer is the main reason for a substantial number of deaths in developing countries and has been reported to be one of the deadly

cancers throughout the world [1]. This disease is responsible for 0.331 million deaths every year. Accounting for 4% of the cancer-related deaths, pan-

Correspondence to: Yiqun Du, MD. Department of Medical Oncology, Fudan University, Shanghai Cancer Center, 270 Dong'an Road, Shanghai 200032, China.
Tel/Fax: +86 021 64433755, E-mail: danyelssche@yahoo.com
Received: 18/10/2018; Accepted: 12/11/2018

creatic cancer is thought to be the 7th principal cause of cancer related deaths across the world [2]. With just 5% 5-year survival rate, it is one of the most destructive malignancies [3]. Consequently, markers for early detection, exploration and identification of effective chemotherapeutic agents and post-therapeutic monitoring are of utmost importance.

Plants have been employed by humans for the design and development of drugs in the past and are still used for the isolation of drugs to treat several of the human disorders [4]. Usually, plants synthesize a wide diversity of bioactive compounds to overwhelm stress and to adapt to a challenging environmental condition. These natural chemical compounds, often called as secondary metabolites, have been shown to exert medicinal properties and have been used for the treatment of diseases as deadly as cancer. For example, taxanesetoposide, vincristine, vinblastine and camptothecins are among the common anticancer agents of plant origin [5,6]. Although these secondary metabolites have been chemically categorized into different groups, anthraquinones form an important group with tremendous pharmacological potential. These anthraquinones have been reported to inhibit growth, trigger apoptosis, and exert anti-metastatic effects. These molecules have mainly been shown to act via PI3K, tyrosine kinases, protein kinase C (PKC), NF- κ B and MAPK signaling cascades [7].

This study was designed to examine the anticancer activity of aloe emodin (Figure 1) and its effects on autophagic cell death, apoptosis, mitochondrial membrane potential ($\Delta\Psi$ m) loss and cell cycle arrest in MIAPaCa-2 and PANC-1 human pancreatic cancer cells.

Methods

Chemicals and other reagents

Aloe emodin (95% purity) was purchased from Sigma-Aldrich (Merck KGaA, Darmstadt, Germany). Growth medium (minimum essential medium/RPMI-1640), fetal calf serum (FCS), trypsin, penicillin, streptomycin, dimethyl sulfoxide (DMSO), RNase, RIPA Buffer and

SDS (2.5%) were procured from Hangzhou Sijiqing Biological Products Co., Ltd. (Hangzhou, China). Acridine orange (AO)/propidium iodide (PI), 3-(4,5-dimethylthiazol-2-yl)-2,5-diphenyl tetrazolium bromide (MTT) and Annexin V-fluorescein isothiocyanate (FITC) Apoptosis Detection kit were purchased from the National Institute for the Control of Pharmaceutical and Biological Products (Beijing, China). LC3 antibodies were procured from Cell Signaling Technology, Inc. (Danvers, MA, USA).

Cytotoxicity assay for evaluation of cell proliferation

The antiproliferative activity of aloe emodin was measured via MTT assay. MIAPaCa-2 and PANC-1 cells at the density of 1×10^5 cells/well were seeded in 96-well plates and kept overnight in an incubator under standard conditions for attachment. Zero hour plates served as controls. Following attachment, aloe emodin was added. Varied doses (0–100 μ M) of aloe emodin were prepared by serial dilution in complete media. Plates were maintained in the incubator for 48 and 72 hrs. MTT dye (20 μ l; 2.5 mg/ml) was added. Plates were then subjected to incubation for 4 hrs. Subsequently, the media were gently decanted and DMSO (150 μ l) was added. The plates were then subjected to agitation for 15 min and optical density (OD)₅₇₀ was taken using a microplate reader. Antiproliferative activity was measured by the formula:

$$\text{Percentage inhibition} = \left(\frac{1 - \text{OD}_{\text{test molecule}} - \text{OD}_{\text{zero hour}}}{\text{OD}_{\text{control}} - \text{OD}_{\text{zero hour}}} \right) \times 100$$

Clonogenic assay

For clonogenic assay, the exponentially growing MIAPaCa-2 cells were collected and subjected to counting with a hemocytometer. After seeding cells (300 cells/well), the plates were subjected to incubation for 48 hrs to permit the cells to adhere and then varied doses (0, 10, 40 and 80 μ M) of aloe emodin were added to the cell culture. Following treatment, the cells were kept at 37°C for 4 days, washed with PBS, and colonies were fixed with methanol and stained with crystal violet for 30 min before being counted under a light microscope.

Inverted phase contrast and fluorescence microscopy assays

To examine the effects of aloe emodin on the cellular morphology of MIAPaCa-2 cells, inverted phase contrast and fluorescence microscopic techniques were employed. For inverted phase contrast microscopy, MIAPaCa-2 cells were cultured in 24-well plates at a density of 2×10^5 cells per well. The cells were exposed to treatment with variable doses of aloe emodin (0, 10, 40, 80 μ M). DMSO 1.5% served as the vehicle control. The cells were then subjected to incubation for 48 hrs and visualized under an inverted phase contrast microscope (magnification, x200; Olympus IX71). For fluorescence microscopy, cells were cultured in 6-well plates and subjected to treatment with 0, 10, 40 and 80 μ M aloe emodin for 48 hrs. The untreated control cells and the aloe emodin-treated cells were incubated with AO/PI (20 μ g/ml each) and then analyzed under a fluorescent microscope (magnification, x200; Olympus IX71).

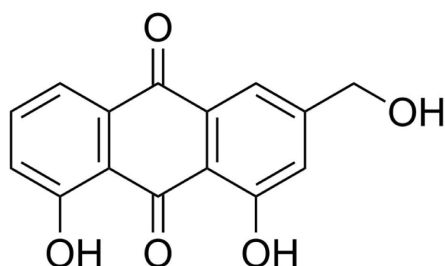


Figure 1. Molecular structure of aloe emodin.

DNA damage assay

For this assay, the MIAPaCa-2 cells were cultured in a 60-mm cell culture plate and subjected to incubation for 48 hrs and subsequently subjected to treatment with 0, 10, 40, 80 μ M aloe emodin for 48 hrs. The cells were collected and PBS-washed, and then the cell pellets were subjected to lysis in a lysis buffer for 50 min. The samples were then centrifuged at $12,000\times g$ at 4°C and the supernatant was prepared in an equal volume of 2.5% SDS and incubated with 10 mg/ml RNase A for 4 hrs. Finally, DNA was dissolved in gel loading buffer, and separated by electrophoresis in agarose gel (1.2%), stained with ethidium bromide and examined under an ultraviolet microscope.

Annexin V-FITC/PI assay for apoptosis detection

Briefly, MIAPaCa-2 cells were cultured in 6-well plates at a density of 2×10^5 cells/ml and then subjected to treatment with 0, 10, 40, and 80 μ M aloe emodin and incubated for 24 hrs. The cells were then collected via trypsinization, and PBS-washed, and resuspended in 200 μ l binding buffer, containing 10 μ l each of Annexin V-FITC and PI. The cells were kept at 37°C for 40 min in the dark and finally the cell samples were examined by flow cytometry.

Evaluation of $\Delta\Psi m$ loss

Flow cytometry in combination with rhodamine-123 dye were used to analyze the effects of aloe emodin on the $\Delta\Psi m$ loss. Briefly, MIAPaCa-2 cells were seeded at a density of 2×10^6 cells/ml and treated with 0, 10, 40 and 80 μ M aloe emodin for 48 hrs. Subsequently, rhodamine-123 dye (10 mM) was added 1 hr before termination of the experiment. The cells were harvested by trypsinization, washed with PBS and incubated with PI (10 μ g/ml) for 30 min at room temperature. The $\Delta\Psi m$ was then measured using flow cytometry (FACS Calibur; BD Biosciences, Qume Drive San Jose, CA, USA).

Cell cycle analysis using flow cytometry

In brief, MIAPaCa-2 cells were cultured at a density of 2×10^6 cells per well and subjected to incubation at 37°C for 12 hrs. The medium was substituted with fresh DMEM comprising of various doses of aloe emodin and further incubated at 37°C for 24 hrs. The treated and untreated cells were then collected, PBS-washed and fixed using 70% methanol for 20 min. After fixing, the cells were washed again with ice-cold PBS, and stained with 20 μ g/ml PI, while 10 μ g/ml RNase A was added for 20 min. Finally, using a FACS Calibur flow cytometer, cell cycle analysis was performed and the data was analyzed using cell cycle analysis software.

Detection of autophagy using western blot assay

Aloe emodin-treated cells were washed twice in ice-cold PBS and then extracted with RIPA buffer, comprising a mixture of 5% each of phosphate and protease inhibitor. The cell lysates were centrifuged at $12,000\times g$ for 20 min at 4°C and protein concentrations were estimated using Bio-Rad protein assay. Twenty μ l from each

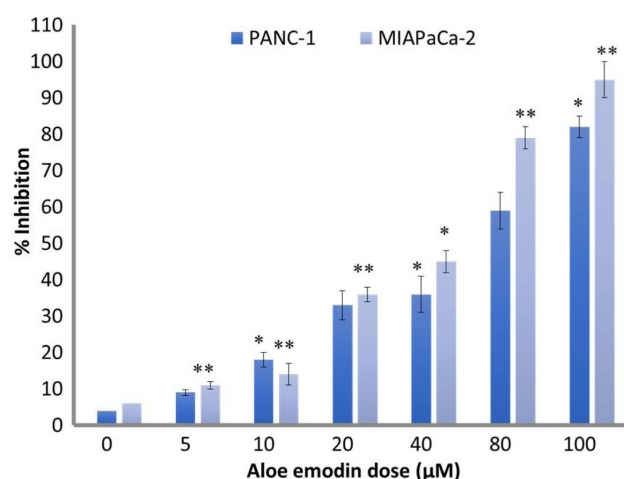


Figure 2. Aloe emodin induces growth inhibitory effects in MIAPaCa-2 and PANC-1 human pancreatic cancer cells. The cells were exposed to various doses (0, 5, 10, 20, 40, 80 and 100 μ M) of aloe emodin for 48 h. Data are shown as mean \pm SD of three independent experiments. * $p < 0.05$, ** $p < 0.01$ vs 0 μ M (control).

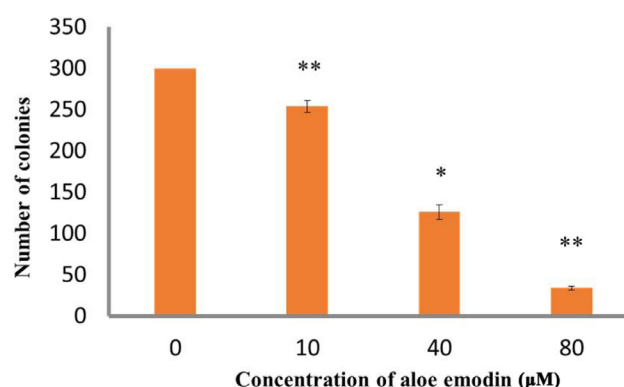


Figure 3. Aloe emodin treatment led to reduction in the number of colonies of MIAPaCa-2 human pancreatic cancer cells. The cells were exposed to various doses (0, 10, 40 and 80 μ M) of aloe emodin for 48 h. Data are shown as mean \pm SD of three independent experiments. * $p < 0.05$, ** $p < 0.01$ vs 0 μ M (control).

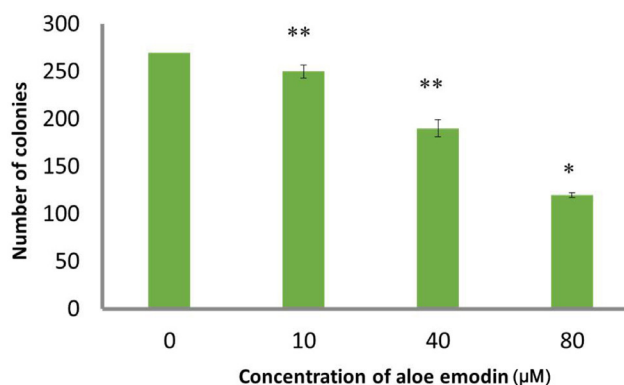


Figure 4. Aloe emodin treatment led to reduction in the number of colonies of PANC-1 human pancreatic cancer cells. The cells were exposed to various doses (0, 10, 40 and 80 μ M) of aloe emodin for 48 h. Data are shown as mean \pm SD of three independent experiments. * $p < 0.05$, ** $p < 0.01$ vs 0 μ M (control).

sample were separated by SDS-PAGE and then moved to nitrocellulose membranes. The membranes were then probed with specific anti LC3-I and LC3-II antibodies at 4°C overnight, washed with PBS buffer and incubated at 37°C with horseradish peroxidase-conjugated anti-rabbit for 1 hr. The bands were visualized using an ECL chemiluminescent detection kit.

Statistics

The results are presented as mean \pm standard deviation values from three independent experiments. Differences between the groups were examined by Student's *t*-test using SPSS 17.0 software (SPSS, Inc., Chicago, IL, USA). $P < 0.05$ was considered to indicate a statistically significant difference.

Results

Aloe emodin inhibits cell proliferation and clonogenic survival in MIA-PaCa-2 and PANC-1 cells

The MTT results showed that aloe emodin (Figure 1) exerts potent cytotoxic effects in MIA-PaCa-2 and PANC-1 cancer cells (Figure 2) and these effects were found to be concentration-dependent. MIA-PaCa-2 cancer cells showed higher degree of growth inhibition and low values of IC_{50} as compared to PANC-1 cells. Further clonogenic assay experiments were used to evaluate the impact of the compound on colony formation. The results (Figure 3 and Figure 4) demonstrated that aloe emodin led to concentration-dependent inhibition of colony formation. Here again the MIA-PaCa-2 cancer cells exhibited significantly more inhibi-

tion of cell colonies with increasing dose, while as PANC-1 cells showed lesser inhibition of colony formation (Figure 4).

Aloe emodin led to morphological changes in MIA-PaCa-2 cells

Inverted phase contrast microscopy was performed to examine the effects of various doses of aloe emodin on the cellular morphology of MIA-PaCa-2 cells. The findings, which are presented in Figure 5, demonstrated that the untreated control cells showed normal cell morphology without any cell shrinkage, while the aloe emodin-treated cells exhibited cell shrinkage along with distortion of the normal cell morphology. This effect was enhanced with increasing doses of the drug.

Aloe emodin induced apoptosis-associated morphological changes in MIA-PaCa-2 cells

Using AO/PI double-staining along with fluorescence microscopy, the impact of aloe emodin on the induction of apoptosis in MIA-PaCa-2 cells was investigated. The results (Figure 6) demonstrated that unlike untreated control cells, which revealed normal cellular morphology and emitted green fluorescence, aloe emodin-treated cells at 10, 40 and 80 μ M doses revealed marked changes in cellular morphology, including cellular shrinkage, membrane blebbing and chromatin condensation. Aloe emodin-treated cells predominantly emitted red/orange fluorescence, which is indicative of apoptosis. The fraction of cells that emit red fluo-

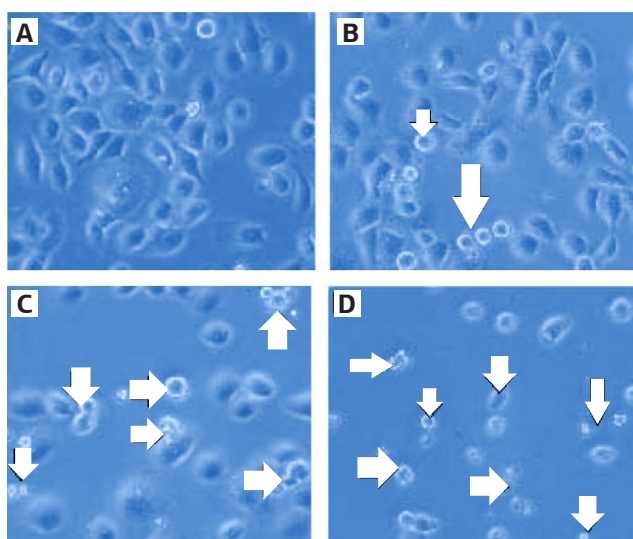


Figure 5. Inverted phase contrast microscopic images of the MIA-PaCa-2 pancreatic cancer cells after treatment with increasing doses (0 (A), 10 (B), 40 (C) and 80 (D) μ M) of aloe emodin. Arrows represent the deformed cells. Untreated control cells (A) show normal cell morphology as compared to the aloe emodin-treated cells (B-D).

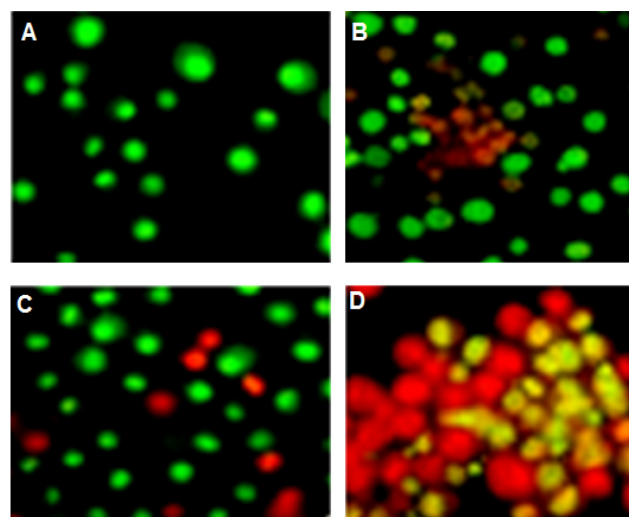


Figure 6. Aloe emodin induces apoptosis in MIA-PaCa-2 pancreatic cancer cells after treatment with various doses (0 (A), 10 (B), 40 (C) and 80 (D) μ M) of aloe emodin for 48 h. The cells were stained with acridine orange/propidium iodide and then analyzed under a fluorescence microscope at 400 \times magnification. The apoptotic cells are indicated by orange and yellow colored cells.

rescence was observed to increase with increasing doses of aloe emodin, indicating that the fraction of apoptotic cells also increased with the dose of the drug.

Aloe emodin led to DNA fragmentation

Using gel electrophoresis, which involves DNA ladder formation, the DNA damaging effects of aloe emodin in MIA-PaCa-2 cells were evaluated. It was observed that aloe emodin-treated cells showed significant DNA ladder formation as compared to control (Figure 7) and this effect increased dose-dependently. This indicates that in the control group, the DNA of the cells remained intact, while in the aloe emodin-administrated cells, DNA fragmentation occurred that led to cell death.

Aloe emodin induced early and late apoptosis

The Annexin V-FITC assay was used to quantify the cells in the early and late apoptotic stages. The results of this assay demonstrated that aloe

emodin induces early and late apoptosis in MIA-PaCa-2 cells. The untreated control cells showed only 3.9% of cells in the early apoptotic stage and 2.5% of cells in the late apoptotic stage (Figure 8A). However, cells treated with 10, 40 and 80 μ M aloe emodin showed that the early apoptotic cell percentage augmented to 17.5, 39.6 and 58.8%, respectively while, the late apoptotic cell percentage increased to 22.3, 27.6 and 37.2%, respectively (Figure 8B-D). Q1-4 represented necrotic, late apoptotic, viable and early apoptotic cells, respectively.

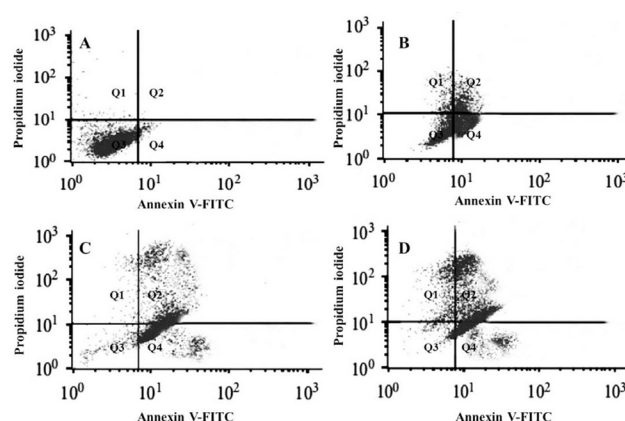


Figure 8. Annexin V-FITC assay for determining the apoptosis induction in MIA-PaCa-2 cancer cells after treating with different doses (0 (A), 10 (B), 40 (C) and 80 (D) μ M) of aloe emodin for 48 h and then analyzed by flow cytometry. Q1, Q2, Q3 and Q4 represent necrotic cells, late apoptotic cells, viable cells and early apoptotic cells respectively.

Aloe emodin dose (μ M)

0 (Con) 10 40 80

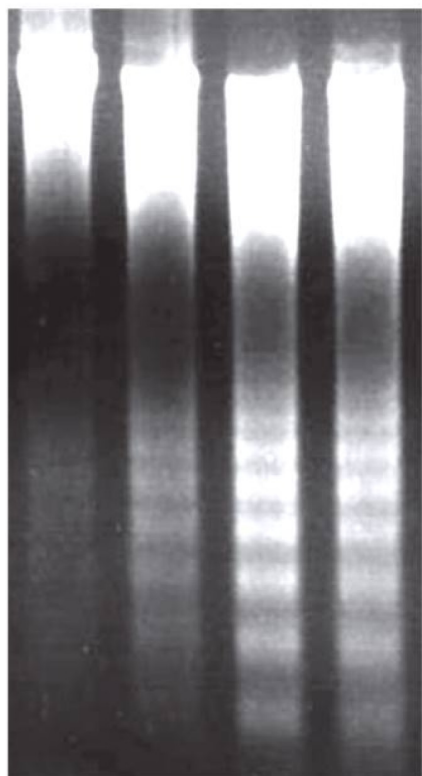


Figure 7. DNA ladder formation induced by treating MIA-PaCa-2 pancreatic cancer cells with varying doses (0, 10, 40 and 80 μ M) of aloe emodin for 48 h and then analyzed by agarose gel electrophoresis. Untreated control did not show any DNA ladder formation.

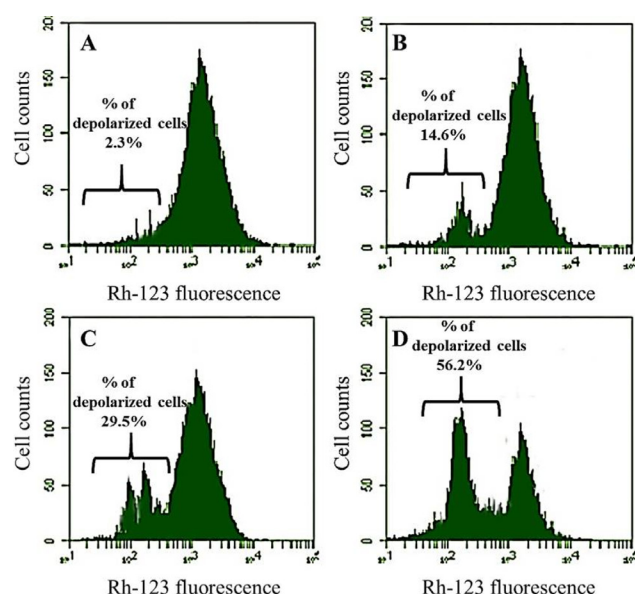


Figure 9. Aloe emodin induced mitochondrial membrane potential loss ($\Delta\Psi_m$) in MIA-PaCa-2 pancreatic cancer cells after treating cells with 0 (A), 10 (B), 40 (C) and 80 (D) μ M of aloe emodin for 48 h. The cells were then stained with Rh-123 fluorescent probe and finally analyzed by flow cytometry. The percent of cells with depolarized mitochondria increased with increasing doses of the drug.

Aloe emodin led to $\Delta\Psi_m$ loss in MIA-PaCa-2 cells

To further investigate the underlying mechanism of the anticancer action of aloe emodin, flow cytometry along with rhodamine-123 dye was used to evaluate the effects of the compound on $\Delta\Psi_m$. The current findings (Figure 9A-D) demonstrated that aloe emodin at increasing doses (10, 40 and 80 μM) tended to induce $\Delta\Psi_m$ loss. In comparison to control group, in which only 2.3% of cells

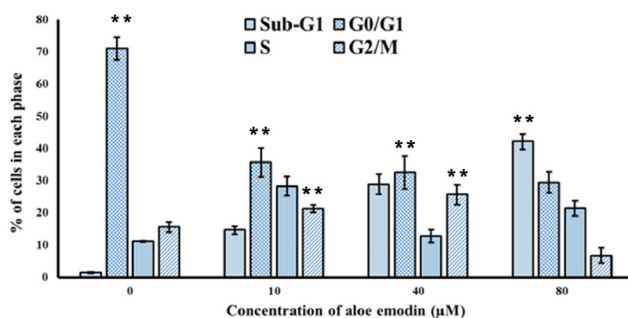


Figure 10. Aloe emodin led to sub- G_1 cell cycle arrest in MIA-PaCa-2 cells after treating cells with indicated doses of aloe emodin for 48 hrs, followed by addition of propidium iodide as a DNA staining agent. The cells were then analyzed by flow cytometry. The percent of sub- G_1 phase (apoptotic cells) cells increased from 1.9% in control to 15.6%, 27.2% and 41.5% in 10, 40 and 80 μM aloe emodin-treated cells, respectively (** $p < 0.01$).

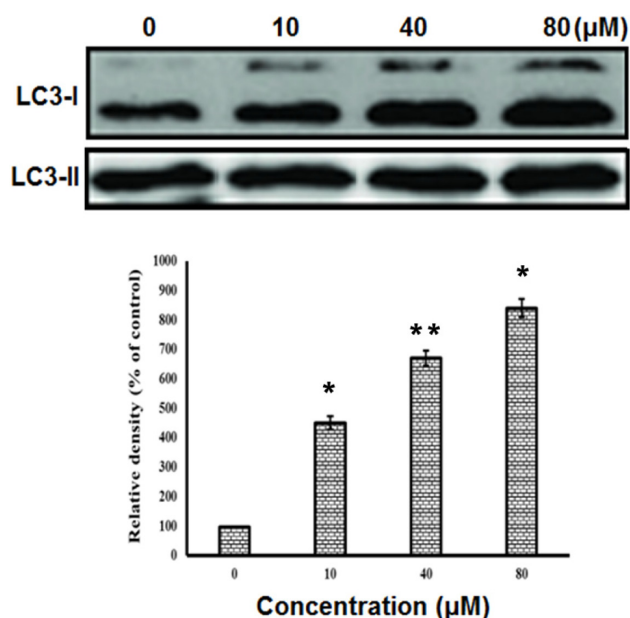


Figure 11. Aloe emodin led to autophagy induction in MIA-PaCa-2 cells after treatment with 0, 10, 40 and 80 μM dose of aloe emodin for 48 h. Western blot assay was used to study the conversion of LC3-I to LC3-II using specified antibodies. The transformation of LC3-I to LC3-II which is considered to be the signpost of induction of autophagy, was seen after the dose of the drug was increased from 10, 40 to 80 μM . (* $p < 0.05$, ** $p < 0.01$).

had depolarized mitochondria (loss of $\Delta\Psi_m$), in the aloe emodin-administered cells with 10, 40 and 80 μM dose, the percentage of cells with depolarized mitochondria increased to 14.6, 29.5 and 56.2%, respectively. Thus, aloe emodin triggered apoptosis via the mitochondrial signaling pathway.

Aloe emodin induces sub- G_1 cell cycle arrest in MIA-PaCa-2 cells

Flow cytometry revealed that aloe emodin also exerted potent effects on the cell cycle phase distribution. In comparison to the untreated cells, aloe emodin-treated cells showed an increase in the fraction of cells in the sub- G_1 phase. The percent of sub- G_1 phase cells increased from 1.9% in control to 15.6, 27.2 and 41.5% in 10, 40 and 80 μM aloe emodin-treated cells, respectively. The results of this assay are presented in Figure 10. Of note, the higher the cell counts in the sub- G_1 phase, the higher the fraction of apoptotic cells. In addition, the fraction of G_2/M cells increased with increasing drug dose.

Aloe emodin induced autophagy in MIA-PaCa-2 cells

As aloe emodin also led to autophagic cell death in these cells, western blot assay was performed to demonstrate the impact of aloe emodin on the conversion of light chain 3 (LC3)-I to LC3-II. Previously, LC3 has been shown to be key in autophagic induction. It has been reported that during autophagy, transformation of LC3-I to LC3-II occurs and this transformation is easily tracked via western blot assay [8]. The current results indicated that aloe emodin treatment led to a marked enhancement of the conversion of LC3-I to LC3-II and this increase was demonstrated to be dose-dependent (Figure 11). Thus, it appears that aloe emodin induces autophagy by modifying LC3 expression levels.

Discussion

In the current study, the antitumor effects of aloe emodin, a naturally occurring anthraquinone compound, on MIA-PaCa-2 and PANC-1 human pancreatic cancer cells were investigated. In addition, the effects of this compound on triggering of apoptosis, cell cycle phase distribution, the $\Delta\Psi_m$ and autophagy were evaluated. Initially, MTT assay and clonogenic assays were carried out to examine the impact of aloe emodin on cell viability and colony formation tendency, which indicated that this compound induced potent cytotoxic effects, along with inhibiting the colony formation efficacy of these cells. Furthermore, using inverted phase contrast

and fluorescence microscopic techniques, it was demonstrated that aloe emodin induced significant cell morphological alterations, such as cell shrinkage, membrane blebbing, chromatin condensation and other changes. Gel electrophoresis demonstrated that aloe emodin led to DNA fragmentation and this effect was dose-dependent. The flow cytometric experiments revealed that aloe emodin induced early, as well as late apoptosis in addition to inducing loss of $\Delta\Psi_m$. Aloe emodin was reported to trigger sub- G_1 cell cycle arrest. The current results revealed that, in addition to inducing apoptosis, aloe emodin treatment induced autophagy. The results demonstrated that aloe emodin treatment led to a marked enhancement of the switch of LC3-I to LC3-II. During autophagy, transformation of LC3-I to LC3-II occurred and this transformation was demonstrated by western blot assay [8,9].

Autophagy induction in cancer cells is a novel and efficient therapeutic strategy to treat cancer. There are various studies which suggest that various anticancer drugs induce autophagy, including temozolomide, etoposide, doxorubicin, epirubicin, As_2O_3 , tamoxifen and many histone deacetylase inhibitors [10-13]. Aloe emodin is an anthraquinone and a variety of emodin present in aloe latex, an exudate from the aloe plant. Aloe emodin has

been reported to be a different kind of antitumor compound which shows selective anticancer action against neuroectodermal tumors [14]. This molecule has also been reported to exert anticancer effects in a new Merkel carcinoma cell line [15]. In another study, it was reported that aloe emodin could potentiate the antitumor effects of some clinically used anticancer drugs including cisplatin (abiraterone), doxorubicin (adriamycin), and 5-fluorouracil etc in an adherent variant cell line of Merkel cell carcinoma [16].

In conclusion, with regard to the role of natural compounds in the development of anticancer drugs [17], the current study demonstrates the anticancer activity of aloe emodin in MIA-PaCa-2 and PANC-1 human pancreatic cancer cells along with showing its effects on apoptosis induction, cell cycle arrest, DNA fragmentation and autophagy induction in MIA-PaCa-2 cells. Taken together, our results clearly indicate that aloe emodin could prove an important lead molecule for the management of pancreatic cancer and deserves further *in vivo* evaluation.

Conflict of interests

The authors declare no conflict of interests.

References

1. Ilic M, Ilic I. Epidemiology of pancreatic cancer. *World J Gastroenterol*. 2016;22:9694.
2. Zhang Q, Zeng L, Chen Y et al. Pancreatic cancer epidemiology, detection, and management. *Gastroenterol Res Pract* 2016;2016:8962321.
3. Kamisawa T, Wood LD, Itoi T, Takaori K. Pancreatic cancer. *Lancet*. 2016;388:73-85.
4. Shakya AK. Medicinal plants: future source of new drugs. *Int J of Herbal Med* 2016;4:59-64.
5. Santhosh RS, Suriyanarayanan B. Plants: a source for new antimycobacterial drugs. *Planta Medica* 2014;80:9-21.
6. Howes MJ. The evolution of anticancer drug discovery from plants. *Lancet Oncol* 2018;19:293-4.
7. Huang QI, Lu G, Shen HM, Chung MC, Ong CN. Anticancer properties of anthraquinones from rhubarb. *Med Res Rev* 2007;27:609-30.
8. Akar U, Chaves-Reyez A, Barria M et al. Silencing of Bcl-2 expression by small interfering RNA induces autophagic cell death in MCF-7 breast cancer cells. *Autophagy* 2008;4:669-79.
9. Hofius D, Schultz-Larsen T, Joensen J et al. Autophagic components contribute to hypersensitive cell death in *Arabidopsis*. *Cell* 2009;137:773-83.
10. Dalby KN, Tekedereli I, Lopez-Berestein G, Ozpolat B: Targeting the prodeath and prosurvival functions of autophagy as novel therapeutic strategies in cancer. *Autophagy* 2010;6:322-9.
11. de Medina P, Payré B, Boubekour N et al. Ligands of the antiestrogen-binding site induce active cell death and autophagy in human breast cancer cells through the modulation of cholesterol metabolism. *Cell Death Differ* 2009;16:1372-84.
12. de Medina P, Silvente-Poirot S, Poirot M. Tamoxifen and AEBs ligands induced apoptosis and autophagy in breast cancer cells through the stimulation of sterol accumulation. *Autophagy* 2009;5:1066-7.
13. Sun WL, Chen J, Wang YP, Zheng H: Autophagy protects breast cancer cells from epirubicin-induced apoptosis and facilitates epirubicin-resistance development. *Autophagy* 2011;7:1035-44.
14. Pecere T, Gazzola MV, Mucignat C et al. Aloe-emodin is a new type of anticancer agent with selective activity against neuroectodermal tumors. *Cancer Res*. 2000;60:2800-4.

15. Wasserman L, Avigad S, Beery E, Nordenberg J, Fenig E. The effect of aloe emodin on the proliferation of a new Merkel carcinoma cell line. *Am J Dermatopathol* 2002;24:17-22.
16. Fenig EI, Nordenberg J, Beery E, Sulkes J, Wasserman L. Combined effect of aloe-emodin and chemotherapeutic agents on the proliferation of an adherent variant cell line of Merkel cell carcinoma. *Oncol Rep* 2004;11:213-7.
17. Liu JJ, Zhang L, Lou JM, Wu CY. Chalcone derivative, chana 1 induces inhibition of cell proliferation and prevents metastasis of pancreatic carcinoma. *Adv Biomed Pharma* 2015;2:115-9.